IJISET - International Journal of Innovative Science, Engineering & Technology, Vol. 4 Issue 8, August 2017
ISSN (Online) 2348 – 7968 | Impact Factor (2016) – 5.264
www.ijiset.com

Graphene Nanoparticles and Graphene Nanoparticles - Polyamide 12/12 Composites

Yurii Sementsov[1,2], Stanislav Makhno[2], Mykola Kartel[1,2], Wang Bo[1], Galina Dovbeshko[3], Volodymyr Styopkin[3] and Sergiy Nedilko[4]

China-Central and Eastern Europe International Science and Technology Achievement Transfer Center, Ningbo University of Technology, Ningbo, 315211, China

[2]Department of Nanoporous and Nanosized Carbon Materials, O. Chuiko Institute of Surface Chemistry, NASU, Kyiv, 03164, Ukraine

[3]Department of Physics of Biological Systems, Institute of Physics, NASU, Kyiv, 03028, Ukraine

[4]Optics Department of Taras Shevchenko Kyiv National University, Kyiv, 01033, Ukraine

Abstract

Graphene nanoparticles (GNPs) have been prepared by means of an anodic oxidation of thermally exfoliated graphite foil. Using this method, GNPs with adjustable characteristics and the particle size ranges, from tens to hundreds of nanometers and from few to tens of micrometers are obtained. The synthesized particles are the nanoscaled multi-layered (5-10 layers) graphene particles as confirmed by Raman spectroscopy, scanning electron microscopy, x-ray diffraction and thermogravimetric analysis. The formed films consist of 75% of GNPs and polycrystalline graphite for the rest. GNPs exhibited the ability to be self-organized in the flower-like structures. The stable aqueous suspensions of GNPs revealed the photoluminescent (PL) activity. PL spectra of the colloids are complex and consist of two components - green-yellow and red. The properties of the composites based on polyamide 12/12 containing GNPs (up to 0.06 volume fraction) are investigated. As shown by DTA, the increase of GNPs content leads to the decrease of the melting point of the polymer and to the increase of polymer destruction. The dependences of the concentrations on i) conductivity at low frequencies and ii) real and imaginary parts of the complex dielectric permittivity of composites at 9 GHz frequency are nonlinearly changed in the concentration range of 0.005-0.03 of volume fraction. It points on the presence of percolation threshold at 0.011 of GNPs volume fraction. The critical exponents of percolation theory for the given system are calculated. The results of impedance spectroscopy indicated that the conductivity of initial GNP is mainly caused by electronic item.

Keywords: *Graphene Nanoparticles (GNPs), GNPs Suspensions, GNPs Films, Anodic Oxidation, Raman Spectra, Photoluminescence (PL), GNPs - Polyamide 12/12 Composites.*

1. Introduction

Graphene nanoparticles (GNPs) consisted of two or more layers (up to ten) as well as graphene monolayer possess the unique physical and chemical properties. Therefore, they are widely investigated as individual particles in the form of continual films and as fillers for polymeric materials [1-3]. Such materials exhibited higher stability in comparison with one-layered graphene and are useable for large-scale manufacturing according to the scheme "top down". This scheme is based on the splitting of different compounds with graphite-like structure using various methods [1-3]. The incorporation of GNPs in polymers leads to the significant increase of the dielectric constant [4], the change of thermodynamic properties of the composite [5], the increase of the crystallinity degree and the resistance to thermal degradation [6]. In addition to, the synergetic increase in absorption of electromagnetic radiation provided by an interaction with carbon nanotubes in porous system polydimethylsiloxane [7]; the increase of tensile strength to 21% for biothermoplastic materials at its low concentrations [8] are also caused by the presence of GNPs. Modification of synthetic polymer fibers by graphene nanoparticles yields a number of improvements and an appearance of new properties, such as adsorption performance, antibacterial character, hydrophobicity and conductivity that are useful for wide range of applications [9]. In this study, the specific parameters of GNPs obtained by anodic oxidation of thermally exfoliated graphite foil, GNPs containing stable colloids and GNPs - polyamide 12/12 composites are characterized in detail.

2. Materials and Methods

For the production of GNPs, one of the most effective methods was used, as namely the anodic oxidation of thermally exfoliated graphite (TEG) foil (Ukraine standard - TU 26.8-30969031- 002-2002) in the low concentrated aqueous KOH solution [10]. As a precursor for TEG, the intercalated graphite compounds (IGC) (Ukraine standard - TU 14.50.9-30969031-001-2002) obtained by anodic oxidation of natural graphite were applied. Such procedure of two consecutive controlled electrochemical processes allowed to initially adjusting the defective structure of the TEG as the cluster-assembled nanoscale systems [11], and further, the size and surface state of GNPs [10]. The GNPs sizes estimated by Laser Correlation Spectroscopy (LCS) (a "ZetaSizer 3" spectrometer (Malvern Instrument, UK) with correlation 7032 and a helium-neon laser LH-111 stated a capacity of 25 mW at λ = 633 nm). The particle sizes in GNPs stable aqueous dispersions were found to be in the range of tens - hundreds of nanometers and few - tens of micrometers and can be regulated within the certain limits [10]. A software in the appropriate mode CONTIN ("multimodal") was used to determine the particle distribution according to the amount of particles with certain size and the volume (in the case of constant mass density) in the approximation of the spherical shape of the particles [12].

Nanoscale dimensionality of GNPs was detected from the Raman spectra (a Brucker RFS 100/s spectrometer, the radiation source was an argon laser, λ = 514.5 nm) and the images of a scanning electron microscopy (SEM) (JSM-35, JEOL). The nanoscale size of the particles was also confirmed by X-ray analysis (a diffractometer DRON-4-07, CuKα radiation, Nickel filter in the reflected beam) in Bragg–Brentano geometry.

Polyamide -12/12 ($PA_{12/12}$) filled with GNPs was obtained by the following procedure: polymer in the powder form was added to the stable dispersion of GNPs, then the mixture was dispersed in an ultrasonic bath for 2 min, dried at 350 K and pressed at 450 K and 5MPa.

Thermogravimetric measurements, as namely the weight loss (TG) and differential thermal analysis (DTA) were carried out using a "Derivatograph Q-1500 D (Hungary) in a static air atmosphere. A sample with the mass of 100 mg was heated from room temperature to 1273 K at 10 K/min heating rate in a ceramic crucible.

The photoluminescence (PL) emission and excitation spectra were measured by means of a single-grating (1200 grooves/mm) registration monochromator MDR-2 (the linear dispersion is 0.5 mm/nm) or DFS-4 (the linear dispersion is 1 mm/nm) equipped with a FEU-100 or FEU-79 photomultipliers, respectively. MDR-2 single-grating (1200 grooves/mm, the linear dispersion is 0.25 mm/nm) and double-prism DMR-4 (dispersion is in the range of 0.5 - 0.05 mm/nm) monochromators were also used for mentioned aims exciting light. A nitrogen gas laser with the excitation wavelength (λ_{ex} = 337.1 nm), two diode-pumped lasers (λ_{ex} = 473 and 532 nm, respectively) and Xenon lamp (DKsSh-150) were used as PL excitation sources. The PL spectra were examined as a function of the excitation wavelength and were carried on in the wide region of excitation and emission wavelengths (225-600 and 350-800 nm), respectively. The temperature of a sample was about 300 K (room temperature, RT).

The dependence of complex electric conductivity of the composites on the frequency was determined by means of the calculations of the impedance spectra within the frequency range of 10^{-2} - 10^{6} Hz obtained by a Solartron SI 1260 impedance spectrometer. Conductivity at low frequencies (0.1, 1 and 10 kHz) was recordered by a double-contact method using immittance measurer E7-14.

To measure the real (ε') and imaginary (ε'') parts of complex dielectric permittivity of the composites in the ultrahigh frequency (UHF) in the range of 8-12 GHz, an interferometer with a phase difference RFK2-18 measurer and a R2-60 measurer of standing wave ratio and deamplification with electrodeless technique were applied [13].

3. Results and Discussion

As clearly seen from (Fig.1 a, b), GNPs dried from the low concentrated aqueous suspension on the gold and glass substrates were able to be self-organized in the flower-like structures.

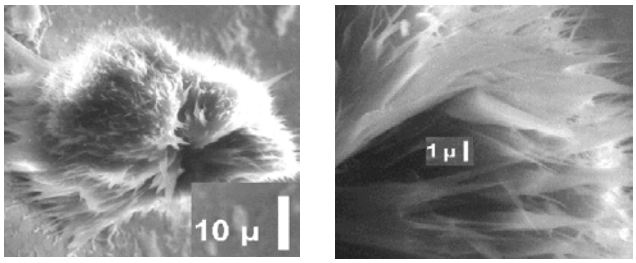

a **b**

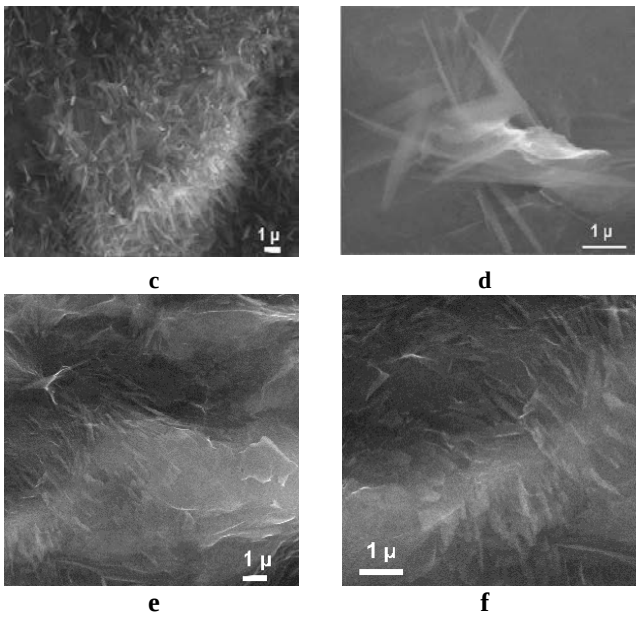

Fig. 1 SEM images of GNPs: a, b – on the gold substrate; c-f – the continual films; c, d – dried in the air; e, f –dried under vacuum in the limited volume.

In the case of the high concentrated dispersion, the solid films of complex structure were formed (Fig.1 c-f). Moreover, the morphology of surface became to be more textured with the formation of distinct GNPs depending on the drying conditions: the surface was smoother after drying in the air (Fig. 1 c, d) and infusion "pressing" dried under vacuum in the limited volume (Fig. 1 e, f).

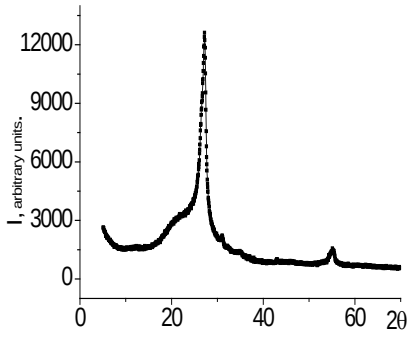

Fig. 2 XRD pattern of GNPs film.

The intensive 2θ peak at 27° related to graphite (002) with a broad shoulder situated at lower 2θ values and the less intensive peak at 55.5°, evidently, corresponded to the second order (004) are presented in the XRD pattern (Fig. 2) of the GNPs film obtained after drying from aqueous dispersion. These lines indicate the presence of polycrystalline graphite. The widening near the main 2θ peak corresponds to the presence of amorphous phase, as namely GNPs of much lower sizes.

Fig. 3 expresses the TG (1) and DTA (2) curves of GNPs films where the temperature 450, 620, 660, 690, 1020 K correspond to the temperature anomalies responsible for the weight decrease of the sample due to the thermal degradation of the certain components. The temperature drop at 450 K is associated with the desorption of chemically bound water whereas the destruction of chemically bound water whereas the destruction of amorphous carbon, the KOH melting and the oxidation of the polycrystalline graphite (large particles) take place at 620 K, 660 K and 1020 K, respectively.

The weight loss (about 18%) in the temperature range of 450-620 K is pointed out the degradation of oxygen-containing functional groups that accompanied by the water and carbon dioxide release according to [8]. At higher temperatures (670-1020 K) the initial weight is decreased on about 50%, as a result of the graphene nanoparticles oxidation. The polycrystalline graphite is only remained (near 17 wt.%) after 1020 K.

Thus, the calcined films (without volatile components) consist of near 75 wt.% of GNPs and graphite particles for the rest as revealed by XRD (Fig. 2) and gravimetric analysis (Fig. 3).

The obtained Raman spectra of GNPs synthesized by us demonstrate the typical Raman shifts for GNPs or graphene multilayers (Fig. 4). A G-band (so called "graphitic" mode of E_{1g} symmetry in Γ-point of Brillouin zone) at 1581 cm^{-1} corresponding to the tangential vibrations of carbon atoms in the rings of graphene sheet [15] is registered. A disorder in the graphene multilayers is characterized by the appearance of D-band at 1353 cm^{-1} taking into account the absent of this band in the initial TEG [16].

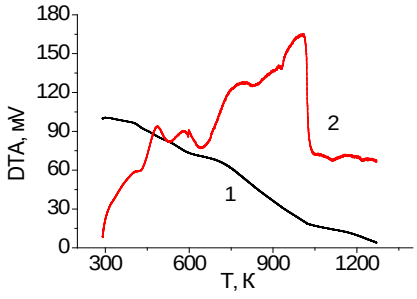

Fig. 3 Dependence of TG (1) and DTA (2) of GNPs films on the temperature.

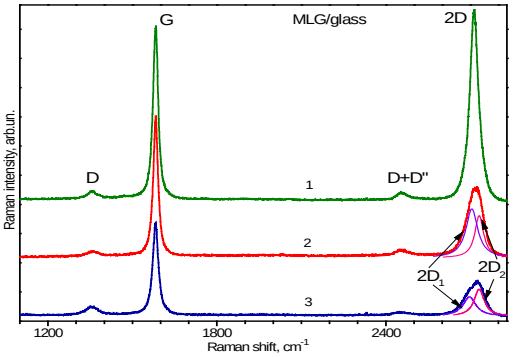

Fig. 4 Raman spectra of GNPs on the glass substrate measured over the different parts of the sample (1, 2, 3).

This Raman peak is assigned to the vibration mode of rings of graphene layer in the K point of Brillouin zone. A relative intensity and half-width (FWHM) of D and G bands reflect a degree of material disorder (the broadening of the bands corresponds to larger degree of disorder).

The second order mode of D vibration (2D band) is registered at 2713 cm^{-1} [17] with higher intensity than usually observed one for the second order vibration. This observation can be an evidence of similarity of carbon nanostructures manifesting a strong electron-phonon interaction and strong dispersion dependence of D-mode. More conductive materials exhibit stronger electron-phonon interaction than semi-conductive ones. A low intensive band at 2451 cm^{-1} called by D" by Vidano and Fischbach [17, 18], consists of the sum of D and D_1 modes (D_1 - sp^3 at 1060-1080 cm^{-1}). In the case of GNPs obtained by us, the position of G-mode at 1581 cm^{-1} does testify the formation of good crystalline structure of GNPs (its theoretical value for graphite and graphene is 1580 cm-1), relative intensity I_{2D}/I_G = 1.12. The analysis of fitted data for 2D mode suggests that the obtained GNPs are of good crystalline structure and exhibit the metal-like conductive properties (inharmonic of 2D mode is about 10 cm^{-1}) [18].

Optical properties. The investigation of optical characteristics was performed for the stable GNPs suspensions (colloids). A colloidal system was filtrated using fritted glass filters with the 1 and 100 μm pore sizes. So, the particle size in the colloids is decreased in the range of initial colloid, after filtration by 100 μm pore size filter and after filtration by 1 μm pore size filter. Hence, tree types of colloidal systems signed, respectively, as C_1, C_2 and C_3 were obtained. It should to note that no sedimentation had been occurred for a half of year.

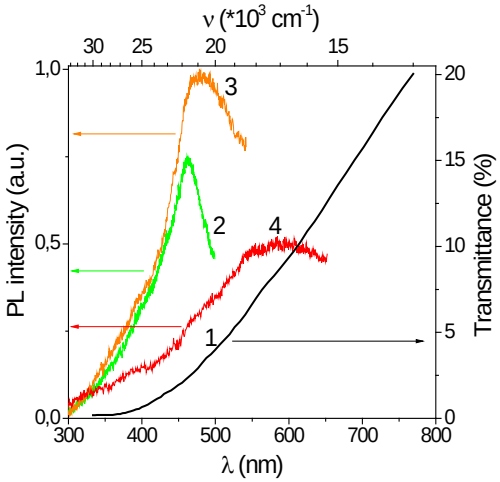

Fig. 5 Transmittance spectrum (1) and PL absorption spectra (2–4) for the C_1 samples. λ_{reg} = 530 (2), 580 (3) and 700 nm (4). T = 300 K.

Absorption of the colloids is measured in the UV-visible range. The optical transmittance spectrum doesn't reveal any peculiarity and shows the monotonic increase of transmittance in the range of 300–800 nm (Fig. 5, curve 1). The view of the curve is typical for graphene containing systems. Any specific feature indicated the presence of the impurities, etc. was not noted on the spectra.

The colloidal samples are characterized with the intensive PL that was easily registered. A wide emission band located in the region of 400–750 nm is observed for the PL spectra of C_1, C_2, and C_3 samples under excitation in the wide range of wavelengths, as namely λ_{ex}: 300 - 532 nm (Fig. 6). The shape and the peak position (λ_{max}) of the PL band are depended on λ_{ex}. Analyzing the PL spectra obtained at different λ_{ex} , it is clear that the position of λ_{max} is shifted to the side of higher wavelength for all tested samples, if λ_{ex} increases (Fig. 6).

IJISET - International Journal of Innovative Science, Engineering & Technology, Vol. 4 Issue 8, August 2017
ISSN (Online) 2348 – 7968 | Impact Factor (2016) – 5.264
www.ijiset.com

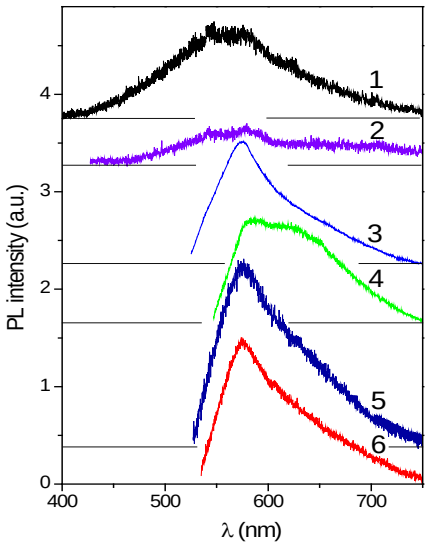

Fig. 6 The PL spectra of C_1 (1–4), C_2 (5), and C_3 samples (6); λ_{ex} = 337.1 (1), 405 (2), 473 (3, 5, 6) and 532 nm (4); T = 300 K.

As seen from PL spectra, the two main components can be distinguished: the first one is a short component (Green – Yellow) in the range from 400 to 700 nm and the second one (Red) appeared from 600 to 800 nm. It is evident that Green–Yellow emission is more pronounced in the spectra. Relative contribution of the bands to the total spectra depends on the λ_{ex}. Excitation of the photoluminescence of the liquids is observed over whole absorption range (see Fig. 5). The increase of wavelength, λ_{reg}, where luminescence was monitored, leads to the shifting of the excitation spectra and their peak position to the longer wavelengths. Whereas, the excitation spectra of Green-Yellow and Red components are obviously different. It indicates on the presence of two main components of GNPs in the colloid. These results are in good agreement with the results of LCS [10].

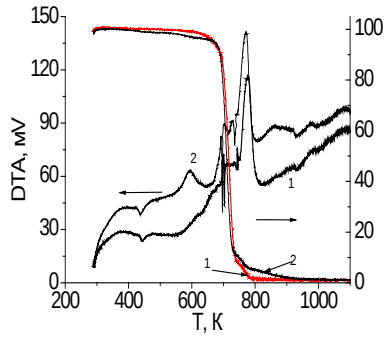

Fig. 7 TG and DTA patterns of PA 12/12 (1) and PA 12/12 – 0.03GNPs (0.03 volume fractions of GNPs).

The properties of composites based on polyamide 12/12 containing GNPs up to 0.06 volume fraction are investigated. DTA patterns of the bare polymer and the composite containing 0.03 volume fraction of GNPs are similar (Fig. 7). The peak near 450 K referred to the polymer melting is shifted by 5 degrees to the side of lower temperatures for a sample containing 0.03 volume fraction of GNPs. Moreover, the appearance of high intensive peak at 598 K observable for PA 1212 - 0.03 GNP is attributed to the destruction of the polymer in the presence of GNPs.

The dependence of conductivity on GNPs volume content (φ) is nonlinear (Fig. 8). The conductivity values at low frequencies are sharply increased by 9 orders at $0 < \varphi < 0.03$ indicating the appearance of percolation threshold. The conductivity value is increased even at 0.006 volume fraction of GNPs. While the conduction channel is appeared at $0.006 < \varphi < 0.03$ due to the formation of the continual lattice from GNPs.

From the analysis of the experimental results, the parameters of percolation equation [9] are determined for the PA12/12 - GNPs system: the percolation threshold φ_s = 0.011, the critical index t = 2.38 and efficient conductivity of GNPs bulk $\sigma_i = 1.36 \cdot 10^1$ $\Omega^{-1} \cdot cm^{-1}$.

The ε 'and ε " values measured for the systems with the different volume contents of GNPs at the frequency of 9 GHz (Fig. 9) are increased with the increase of GNPs content and reached the values of ε' = 29.8 and ε" = 13 at φ = 0.06.

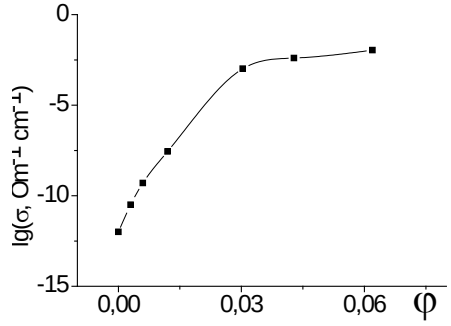

Fig. 8 Logarithm of conductivity *vs* the GNPs volume contents (φ) at 1 kHz for PA 12/12 – GNPs system.

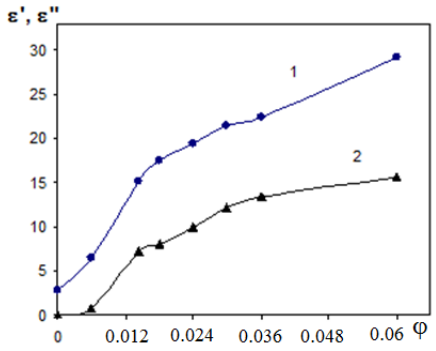

Fig. 9 Dependence of real ε' (1) and imaginary ε" (2) parts of the complex permittivity on the volume content of GNPs at frequency 9 GHz for the PA12/12 - GNPs systems.

The increase of the number of dipoles formed from the GNPs clusters and the further increase in their size and quantity leads to the formation of the dimensional lattice causing to more effective interaction with electromagnetic radiation at given frequency and the gradual increase of the dielectric constant values.

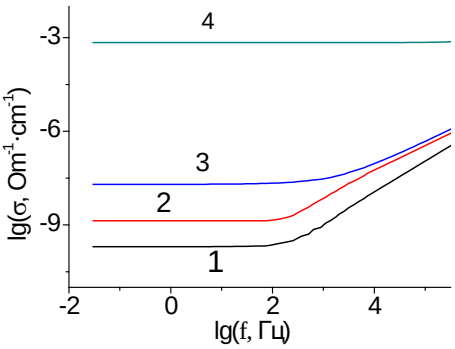

Fig. 10 The dependence of the electrical conductivity logarithm on the frequency for PA12/12 - GNPs composites: 1 – 0.003; 2 – 0.006; 3 – 0.012; 4 - 0.03.

Fig. 10 shows the logarithm of the real component of conductivity for PA12/12 - GNPs composites versus the logarithm of frequency.

The dependence is linear for pure GNPs and independent on the frequency in the range of 10^{-2} - 10^{2} Hz indicating on high electronic conductivity as well as on relatively low ionic conductivity [10]. The gradual increase in conductivity with frequency increasing from 100 Hz and above is fixed for the samples contained less or equal 0.012 of GNPs volume content as a result of the hopping mechanism of conductivity and acceptably described by the equation:

$$\sigma = \sigma_0 \cdot \left(1 + \left(\frac{f}{f_0}\right)^{0.8}\right)$$

where: σ_0 is the initial value of conductivity; f_0 means the frequency corresponded to the change of tangent angle of electrical conductivity on frequency.

The percolation threshold value for the PA 12/12 - GNPs system is twice lower in comparison with the polychlorotrifluoroethylene (PCTFE) - GNPs system. Additionally, the conductivity of the PA12/12 - GNPs system after percolation threshold is higher by five orders than PCTFE system [19] that can be associated with dielectric and adhesion properties of polymers.

4. Conclusions

The comprehensive investigation of the graphene nanoparticles prepared by anodic oxidation of thermally exfoliated graphite foil, their agglomerates, stable dispersions and PA12/12 - GNPs composites contained up to 0.06 volume fraction is considered. It is established that the synthesized nanoparticles are multi-layered graphene particles consisted of 5-10 layers. GNPs are able to be self-organized into "flower-like" dimensional structures.

The GNPs colloids are characterized by intensive PL observed in whole range of absorption. PL excitation spectra of Green-Yellow and Red components are certainly different indicating the presence of two main components of GNPs in the colloid. The conductivity of PA12/12 – GNPs composites points on the high electronic conductivity and relatively low ionic conductivity due to the electronic item of GNPs as revealed the results of the impedance spectroscopy, the electrical conductivity at low frequencies and complex dielectric permittivity in the microwave range. The values of real and imaginary components of complex dielectric permittivity in the ultra-high frequency range and conductivity at low frequencies show the nonlinear dependence on the volumetric fraction of GNPs in PA12/12 – GNPs composites due to the presence of percolation threshold. The percolation threshold for the system is ~ 0.011 volumetric fractions. It is shown that the increase of GNPs content leads to the shift of the melting point of the polymer to lower temperatures and to the increase of polymer degradation.

References:

[1] Sheng Yang, S. Brüller, Zhong-Shuai Wu, Zhaoyang Liu, K. Parvez, Renhao Dong, F. Richard, P. Samorì, Xinliang Feng, and K. Müllen, “Organic radical-assisted electrochemical exfoliation for the scalable production of high-quality graphene”, Journal of the American Chemical Society, Vol. 137, No 43, 2015, pp. 13927–13932.

[2] Vivek Dhand, Kyong Yop Rhee, Hyun Ju Kim, and Dong Ho Jung "A Comprehensive Review of Graphene Nanocomposites: Research Status and Trends", Journal of Nanomaterials, Vol. 2013, ID 763953, 2013, pp. 1-14.

[3] E. D. Grayfer, V. G. Makotchenko, A. S. Nazarov, S. J. Kim, and V. E. Fedorov, "Graphene: chemical approaches to the synthesis and modification", Russian Chemical Reviews, Vol. 80, No 8, pp.751-770.

[4] Ming Tian, Zhaoyang Wei, Xiaoqing Zan, Liqun Zhang, Jing Zhang, Qin Ma, Nanying Ning, and Nishi Toshio, "Thermally expanded graphene nanoplates/ polydimethylsiloxane composites with high dielectric constant, low dielectric loss and improved actuated strain", Composites Science and Technology, Vol. 99, 2014, pp. 37-44.

[5] Ş. İnce, Yo. Seki, M. A. Ezan, A. Turgut, and A. Erek, "Thermal properties of myristic acid/graphite nanoplates composite phase change materials", Renewable Energy, Vol. 75, 2015, pp. 243-248.

[6] F. A. He, H. J. Wu, X. L. Yang, K. H. Lam, J. T. Fan, and H. L. W. Chan "Novel exfoliated graphite nanoplates/ syndiotactic polystyrene composites prepared by solution-blending", Polymer Testing, Vol. 42, 2015, pp. 45-53.

[7] Xinying Sun, Xu Liu, Xi Shen, Ying Wu, Zhenyu Wang, and Jang-Kyo Kim, "Graphene foam/carbon nanotube/ poly (dimethyl siloxane) composites for exceptional microwave shielding", Composites Part A: Applied Science and Manufacturing, Vol. 85, 2016, pp. 199-206.

[8] L. Sisti, J. Belcari, L. Mazzocchetti, G. Totaro, M. Vannini, L. Giorgini, A. Zucchelli, and A. Celli, "Multicomponent reinforcing system for poly(butylene succinate): Composites containing poly(L-lactide) electrospun mats loaded with graphene", Polymer Testing, Vol. 50, 2016, pp. 283-291.

[9] Xuqiang Ji, Yuanhong Xu, Wenling Zhang, Liang Cui, and Jingquan Liu, "Review of functionalization, structure and properties of graphene/polymer composite fibers", Composites Part A: Applied Science and Manufacturing, Vol. 87, 2016, pp. 29-45.

[10] G. I. Dovbeshko, V. S. Kopan, S. L. Revo, M. M. Nishchenko, G. P. Prikhod'ko, M. L. Pyatkovskiy, Yu. I. Sementsov, and M. Vestmayer, "Nanostructure of Exfoliated Graphite" (*in Russian*), Physics of Metals and Advanced Technologies, Vol. 27, No. 3, 2005, pp. 281-289.

[11] M. Kartel, Yu. Sementsov, G. Dovbeshko, L. Karachevtseva, S. Makhno, T. Aleksyeyeva, Yu. Grebel'na, V. Styopkin, Wang Bo, and Yu. Stubrov, "Lamellar structures from graphene nanoparticles produced by anode oxidation", Advanced Materials Letters, Vol. 8, No 3, 2017, pp. 212-216.

[12] U. Ramalinga, J. D. Clogston, A. K. Patri, and J. T. Simpson, "Characterization of Nanoparticles by Matrix Assisted Laser Desorption Ionization Time-of-Flight Mass Spectrometry", in: Characterization of Nanoparticles Intended for Drug Delivery. Methods in Molecular Biology / Ed. S. E. McNeil, Humana Press, 2011, pp. 53-61.

[13] L. M. Ganuk, V. D. Ignatkov, S. M. Mahno, P.M. Soroka. "Study of dielectric properties of the fibrous material" (*in Russian*), Ukrainian Journal of Physics, Vol. 40, No 6, 1995, pp. 627-629.

[14] C. Botas, P. Alvarez, P. Blanco, M. Granda, C. Blanco, R. Santamarıa, L. J. Romasanta, R. Verdejo, M. A. Lopez-Manchado, and R. Menendez, "Graphene materials with different structures prepared from the same graphite by the Hummers and Brodie methods", Carbon, Vol. 65, 2013, pp. 156–164.

[15] R. Nemanich, and S. Solin, "First- and second-order Raman scattering from finite-size crystals of graphite", Physical Review B, Vol. 20, No 2, 1979, pp. 392-401.

[16] G. I. Dovbeshko, O. P. Gnatyuk, A. A. Nazarova, Yu. I. Sementsov, and E. D. Obraztsova, "Vibrational spectra of carbonaceous materials: a SEIRA spectroscopy versus FTIR and Raman", Fullerenes, nanotubes and carbon nanostructures, Vol. 13, No 1, 2005, pp. 393-400.

[17] R. Vidano, and D. Fishbach, "Observation of Raman band shifting with excitation wavelength for carbons and graphites", Solid State Communications, Vol. 39, No 2, 1981, pp. 341–344.

[18] R. Vidano, and D. B. Fischbach, "New bands in the Raman spectra of carbons and graphite", Journal of the American Ceramic Society, Vol. 61, 1978, pp. 13–17.

[19] O. M. Lisova, S. M. Makhno, N. A. Gavrilyuk, G. P. Prikhodko, and M. T. Kartel, "The Electrophysical Properties of Polymer – Graphene Oxide System" (*in Ukrainian*), Surface, Vol. 7(22), 2015, pp. 238-243.
https://surfacezbir.com.ua/index.php/ru/arkhiv-3/26-russkij/sbornik-22/339-22-rus-25-3-8

1) Yurii Sementsov, PhD (Phys. & Math.), Senior Researcher of Physics and Chemistry of Surfaces, Senior Researcher of the Department of Physical Chemistry of Nanoporous and Nanoscale Carbon Materials of the Chuiko Institute of Surface Chemistry of the National Academy of Sciences of Ukraine. He is an expert in the field of nanosized carbon materials with a graphite-like structure and head of the Project from Ukrainian side.

2) Stanislav Makhno, PhD (Phys. & Math.), Senior Researcher of Physics and Chemistry of Surfaces, Head of the Laboratory "Electrophysics of Nanomaterials". He is known due to publications on the synthesis and electrophysical properties of nanocomposites.

3) Mykola Kartel, Dr. Sci. (Chem.), Prof., Academician, Director of the Chuiko Institute of Surface Chemistry of the National Academy of Sciences of Ukraine. The head of the several researches in the field of physical chemistry, in particular, surface chemistry and physics, which are carrying out in the National Academy of Sciences of Ukraine.

4) Wang Bo, Assoc. Prof., PhD (Econ.), Director of China-Central and Eastern Europe International Science and Technology Achievement Transfer Center of Ningbo University of Technology, Ningbo, China.

5) Galina Dovbeshko Dr. Sci. (Phys. & Math.), Prof. The head of the department of Physics of Biological Systems, Institute of Physics, National Academy of Sciences of Ukraine National Academy of Sciences of Ukraine. He is a specialist in the field of spectral methods for studying solid bodies, including nanoscale systems, and their interaction with biological objects.

6) Volodymyr Styopkin PhD (Phys. & Math.), Senior researcher of the department of physical electronics of the Institute of Physics of the National Academy of Sciences of Ukraine, Specialist in electron microscopy

7) Sergiy Nedilko Dr. Sci., (Phys. & Math.), Prof., Head of the Laboratory of spectroscopy of the condensed state of Taras Shevchenko Kyiv National University. He is a specialist in the field of spectroscopy of the condensed state of matter.